Journal of the Serbian Chemical Society
JSCS@tmf.bg.ac.rs • www.shd.org.rs/JSCS
J. Serb. Chem. Soc. *89* (2) 195–213 (2024)
JSCS–5715
Original scientific paper
Published 2 March 2024

The non-ideality in binary aqueous systems contributed to the different abilities of solvent entities incorporated in the solvation shell of methylene blue

SOKAINA S. HEMDAN[1]* and RADWAN ALNAJJAR[2,3]

[1]Department of Chemistry, Faculty of Science and Art El Marj, Benghazi University, El Marj, Libya, [2]Department of Chemistry, Faculty of Science, Benghazi University, Benghazi, Libya and [3]PharmD, Faculty of Pharmacy, Libyan International Medical University, Benghazi, Libya

(Received 12 May, revised 18 June, accepted 1 November 2023)

Abstract: The solvatochromic properties of methylene blue (MB) were investigated in neat water, methanol, ethanol, propanol, dioxane and their corresponding aqueous mixtures. The correlation of the empirical solvent polarity scale (E_T) values of MB with solvent composition was analysed using the solvent exchange model of Bosch and Roses to explain the preferential solvation of the probe thiazine dye in the binary mixed solvents. Non-linear solvatochromism of MB was observed in aqueous mixtures of methanol, ethanol, propanol and dioxane. The influence of the composition of the solvating shell in preferential solvation of the solute dye was investigated in terms of both solvent–solvent and solute–solvent interactions, and the local mole fraction of each solvent composition in the cybotactic region of the probe was also calculated. Effective mole fraction variation can provide important physicochemical insights into the microscopic and molecular interactions between MB species and solvent components. The results showed that the MB solvation shell was thoroughly saturated with the solvent complex S_{12} for dioxane more than ethanol and propanol mixtures, and opposite trends for methanol mixtures, whereas the solvent complex S_{12} could not incorporate into the MB solvation shell. Data from the binary systems were analysed with KAT parameters using a dual model of basicity and polarity. The results showed that the polarity was better suited for spectral shift in aqueous methanol and ethanol solutions, while the basicity was better for aqueous propanol and dioxane solutions.

Keywords: thiazine dye; preferential solvation; aqueous-solvent aggregates; KAT scale.

* Corresponding author. E-mail: Sukains_h@yahoo.com
https://doi.org/10.2298/JSC230512087H

INTRODUCTION

The term solvatochromism is used to explain the pronounced change in position and intensity of the visible absorption peak(s) due to the change of the polarity of the medium when absorption spectra are measured in neat solvents of different polarities.[1] It is found that in addition to the position of the absorption band of the dissolved chromosphere, the intensity and shape are also significantly affected by choice of different solvents, due to the different stabilization of their electronic ground state and excited states.[1] Solvatochromic dyes show significant shifts in absorption wavelength when dissolved in the different solvents.[2,3] The shift is hypsochromic when the shift is to lower wavelengths or bathochromic when the shift is to a longer wavelength. The electronic absorption of organic molecules usually changes when the molecules dissolve in different solvents. This change can also be seen as variations in the absorption spectra' intensity or shape.[4] Solvatochromism is a convenient and straightforward way to study solute–solvent interactions, showing the electrostatic and non-electrostatic solute––solvent interactions.[5,6]

The solution chemistry of binary solvent mixtures is used to understand the effect of the medium on solutes; those solutions can form new solvents with new properties that differ from the neat solvents.[7,8] However, several aqueous protic and aprotic solvent mixtures have similar macroscopic properties(*e.g.*, dielectric constant) but behave very differently from the solvation point.[9] Solute behaviour in binary solvent systems is more complicated than in pure solvents due to the preferential solvation (PS), in which the solute is solvated by one solvent more than the other.[10] Therefore, the solvation shell of the solute is completely saturated with an excess of the more polar solvent compared to the bulk composition, which is related to the preferential solvation. In other words, the preferential solvation occurs when a solute interacts with more molecules of one solvent component in its cybotactic region than the others, compared to the bulk composition. According to the explanation above, the preferential solvation is the key to understanding the solvation in solvent mixing processes. Furthermore, when the preference dominates to the extent that one component is effectively excluded from the solvation shell of the solute, it is called selective solvation.[10] Solvatochromism, which describes the spectral changes of a solute caused by a change in solvent polarity, provides a convenient way to monitor the interactions in the cybotactic region of a solute.[11] In particular, the electronic transition energy of a solute at the absorption maxima, called the polarity scale (E_T), includes all possible interactions between the solute and solvent components, including specific (such as hydrogen bonding and electron donor–acceptor interactions) and non--specific (polarity–polarizability effects) interaction.[12] The changes in absorption maxima follow the changes in solvent composition and E_T values can reveal the nature of the solute–solvent and solvent–solvent interactions in solvent mixing.

Consequently, a solute's E_T parameters can be manipulated to elucidate the preferential solvation phenomena in the mixtures. The $E_{T(30)}$ values for many binary mixtures of molecular and ionic solvents have various models. Both theoretical and experimental methods have been developed for the preferential solvation problem in the literature. Among the theoretical models, models such as the quasi lattice-quasi chemical theory, the Kirkwood–Buff theory, the dielectric enrichment developed by Suppan, the competitive preferential solvation theory of Nagy, and the stepwise solvent exchange model of Covington have been used successfully in a lot of papers.[13–15] The solvent exchange model has been proposed by Bosch and Roses to investigate the preferential solvation experimentally.[16] This model is an extension of Connors's stepwise solvent exchange model, which derives the equations that relate the E_T values of a solute with the solvent composition.[17] In this model, the competition between different solvent––solvent species to solvate the solute is described by some exchange equilibria near the solute.[17] An equilibrium constant, named the preferential solvation parameter, is defined for each exchange reaction, which relates the mole fraction of solvents in the solvation shell to that in the bulk mixture. In addition, the formation of solvating complexes is postulated from solvent-solvent interaction on the microsphere of solvation.

This work describes the solvatochromism of methylene blue in binary aqueous mixtures over the entire composition range, *i.e.*, from neat water to neat cosolvent. The solvents employed include methanol (MeOH), ethanol (EtOH), propanol (PrOH), dioxane and water, the structure of methylene blue, Fig. S-1 of the Supplementary material to this paper. The preferential solvation method was used to interpret the solute–solvent and solvent-solvent interactions. In addition, the spectral shift, λ_{max}, of methylene blue in binary aqueous mixtures was analysed with the linear solvation energy relationship model in two terms KAT parameters for all aqueous mixtures using the SPSS program to obtain more information about the sensitivity of methylene blue to the medium upon change of the mole fraction of cosolvents.

EXPERIMENTAL

Reagents and material

MB was purchased from Merck and applied without purification. The solvents employed, EtOH (96 %), MeOH (99.9 %), PrOH (99.8 %) and dioxane (99.8 %), were all analytical grade and were used without further purification. The used solvents have different polarities mainly related to the refractive index (n) and dielectric constant (ε) of each solvent, which was reported within the literature.[4] The KAT parameter values for all the aqueous organic mixtures used in this work were obtained from the values reported within the literature.[18]

Preparation of solutions and absorption spectra measurements

A 25±0.01 mg quantity of methylene blue was weighed separately and dissolved in some quantity of 96 % ethanol before making up to 25 mL volume in a 25 mL volumetric flask with

the same solvent to give 3.13×10^{-3} mol L^{-1} stock solution of methylene blue. This solution is homogenized and stored in a dark place. Binary mixtures of aqueous methanol, ethanol, propanol and dioxane were prepared by mixing in a volumetric flask the appropriate pure solvents in the volume ratios (water:cosolvent): 0:1.0, 0.2:0.8, 0.3:0.7, 0.4:0.6, 0.5:0.5, 0.6:0.4, 0.7:0.3, 0.8:0.2, and 1.0:0. Adequate equilibrations were allowed before using the solvent mixtures for sample measurements. 0.1 mL of dye stock solute was transferred in a volumetric flask of 10 mL and diluted up to volume by each of the studied binary mixtures in a volumetric flask of 10 mL. The mixtures were homogenized and left to equilibrate before measurement. The visible absorption spectral data were recorded in the appropriate neat solvent and binary mixtures with Cecil-CE 7400 (S.n.146368, England) UV–Vis spectrophotometer model cell, covering the wavelength extending 400–750 nm with a 1.00 cm quartz cell. The distilled water was obtained by using a Gambro distilled water device (AK95 S, Sweden).

Density functional theory (DFT) calculations

Density functional calculations were performed at different levels, including B3LYP[19] levels CAM-B3LYP[20], ωB97XD[21], APFD[22] and M062X[23] combined 6–31+G* basis sets. Further, a full geometry optimization calculation was carried out, followed by frequency calculation, to ensure minimal structures.[24] TD-DFT calculations were carried out in methanol, ethanol, propanol and dioxane. The solvent effects were included using the conductor-like polarizable continuum model (CPCM).[25] All calculations were conducted using Gaussian 16 software.[26]

Data analysis

The spectral characteristics of methylene blue were analysed in numerous binary aqueous organic solvents at a temperature of ~25 °C. The statistical linear regression was performed by using IBM-SPSS (a program of a statistical package of social sciences version 26) to determine coefficients by multiple linear regression techniques.

Preferential solvation (PS) model

Details related to applied model are given in the Supplementary material.

RESULTS AND DISCUSSION

Solvatochromism in binary aqueous systems related to neat solvents

The visible absorption spectra of methylene blue are recorded in several neat solvents with different HBD abilities. Fig. S-2 of the Supplementary material shows the spectra of methylene blue in the neat solvents used in this work. The spectrum in Fig. S-2 exhibits two bands, and the first band is broad and weak. The second band is strong in the wavelength range 650–665 nm, and their λ_{max} values are shifted to higher wavelengths as the dielectric constant of the solutions is increased.[28] The λ_{max} values of MB are red-shifted ($\Delta\lambda$ = 15 nm) when proceeding from dioxane into water solvent. This may be described by the formation of ion-pair species, especially in HBA solvent dioxane with a low dielectric constant.[29] The solvation of MB in HBA solvent dioxane possibly occurs from ion––dipole interactions, whereas in HBD solvents, it is a result of the formation of hydrogen bonding interactions.[28]

Structure optimization, DFT calculations and nature of the frontier molecular orbitals

DFT calculations were used to study the behaviour of MB at a molecular level. The structure of the MB was optimized at B3LYP, CAM-B3LYP, WB97XD, APDF and M062x level of theory combined with a 6-31+G* basis set in the gas phase. The optimized structure is presented in Fig. 1, and critical bond lengths and angles are presented in Table I.

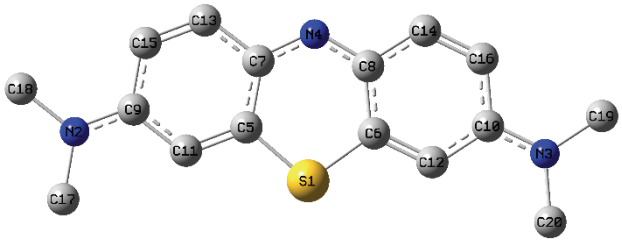

Fig. 1. The optimized structure of MB at B3LYP/6–31+G∗ in the gas phase.

TABLE I. Bond length (Å) and angle (°) at different levels using the 6-31+G* basis set in the gas phase

Bond	B3LYP	CAM-B3LYP	WB97xd	APFD	M062x	Exp[27]
S_1–C_6	1.7509	1.7377	1.7367	1.7372	1.7365	1.729
N_4–C_8	1.3357	1.3287	1.3299	1.3305	1.3302	1.336
N_3–C_{10}	1.3543	1.3458	1.3464	1.3479	1.3441	1.340
N_3–C_{20}	1.4654	1.4590	1.4585	1.4548	1.4592	1.472
C_5–S_1–C_6	103.3057	103.4491	103.4245	103.5806	103.3998	103.80
C_7–N_4–C_8	123.8177	124.0750	123.7826	123.6389	123.6826	123.04
C_{15}–C_9–N_2	120.8189	120.6845	120.6763	120.7437	120.5855	122.03
C_9–N_2–C_{17}	120.5398	120.4203	120.3433	120.5019	120.2480	121.61

As can be seen in Table I, most levels deviated from the experimental bond length of S_1–C_6 by around 0.1 Å, while B3LYP was the most accurate in predicting the C–N bond lengths. Regarding the thiazine ring angles, most levels were able to predict the angle with high accuracy with a deviation of 0.49, 0.35, 0.38, 0.22 and 0.40° observed in the C_5–S_1–C_6 angle for B3LYP, CAM-B3LYP, WB97xd, APFD and M062x, respectively. In the case of the C–N–C angles, most levels predict it with less than 1.00° deviation except for CAM-B3LYP, where a variation of 1.04° was observed.

Using larger bases set (Table II) results in better prediction of the bond lengths, with a deviation in S–C bond of 0.0219, 0.0218 and 0.0206 Å for 6-31+G*, 6-31++G** and 6-311++G**, respectively. In addition, the bond angles in the thiazine ring were predicated more accurately, the C_5–S_1–C_6 angle

predicated to be 103.332° in the case of 6-311++G** which deviates 0.4676° from the experimental finding.

TABLE II. Bond length (Å) and bond angle (°) at B3LYP levels using various basis sets in the gas phase

Bond	6-31+G*	6-31++G**	6-311++G**	Exp[27]
S_1–C_6	1.7509	1.7508	1.7496	1.729
N_4–C_8	1.3357	1.3357	1.3328	1.336
N_3–C_{10}	1.3543	1.3541	1.3515	1.340
N_3–C_{20}	1.4654	1.4655	1.4650	1.472
C_5–S_1–C_6	103.3057	103.3195	103.3324	103.80
C_7–N_4–C_8	123.8177	123.8200	123.9202	123.04
C_{15}–C_9–N_2	120.8189	120.7931	120.7988	122.03
C_9–N_2–C_{17}	120.5398	120.5666	120.6147	121.61

Following the optimization step, time-dependent (TD) DFT was implemented to study the electronic spectra of methylene blue at molecular levels. TD--DFT calculations were carried out at the same levels as the optimization process, and the obtained results are presented in Table III.

TABLE III. The vertical transitions of methylene blue in nm calculated at various DFT levels with 6-31+G* basis set in the gas phase

DFT level	Bond					
	S_0–S_1	S_0–S_2	S_0–S_3	S_0–S_4	S_0–S_5	S_0–S_6
B3LYP	500.61	473.89	382.81	340.49	325.71	289.68
CAM-B3LYP	472.55	412.84	352.62	288.31	286.31	251.90
WB97xd	473.21	412.39	356.17	288.49	282.01	262.01
APFD	492.13	462.05	377.39	331.15	315.38	274.69
M062x	474.13	411.76	369.73	284.84	283.31	262.95
Exp	660					

As can be seen in Table III, the first excited state (S_0–S_1) has the highest oscillator strength, which corresponds to the observed λ_{max}. The deviation in λ_{max} was too high, which indicates that DFT could not reproduce the experimental UV spectra. However, adding the chlorine atom and reoptimizing the structure at B3LYP/6-31+G* in the gas phase incapacitated this deviation, Fig. 2.

The obtained electronic spectra agreed with the experimental finding; the λ_{max} shifted from 500 nm when the chlorine atom was absent to 670 nm in the presence of the chlorine atom, as it can be seen in Fig. 3.

Once a spectrum that is most in agreement with the experimental spectra in the gas phase was obtained, the solvation effect was implemented via the conductor-like polarizable continuum model (CPCM). The obtained electronic spectra are presented in Table IV.

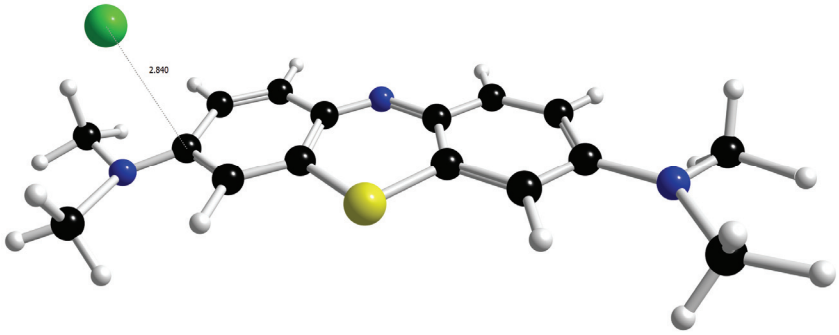

Fig. 2. The optimized structure of MB-Cl at B3LYP/6–31+G* in the gas phase.

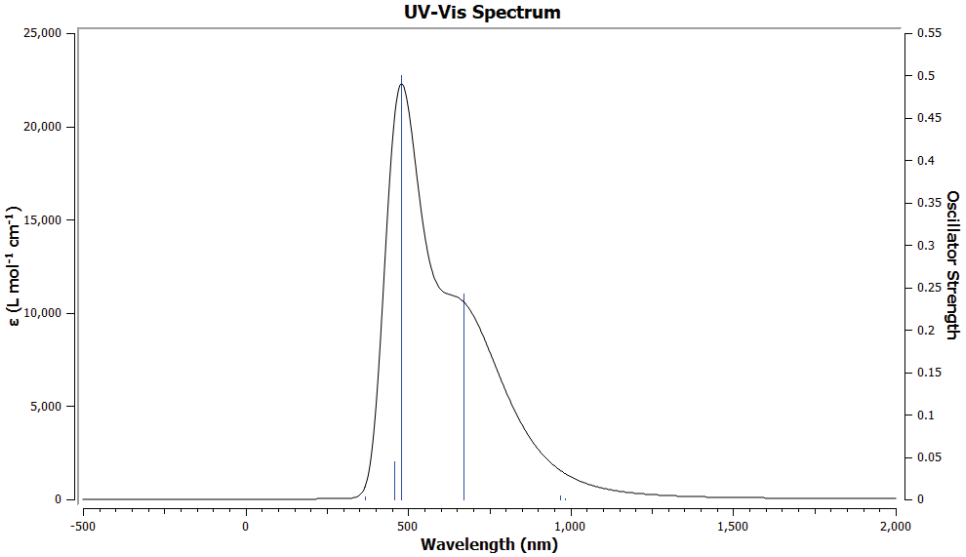

Fig. 3. The electronic spectra of MB-Cl optimized at B3LYP/6-31+G* in the gas phase.

Interestingly, once the solvent effect was implemented, the effect of the chlorine atom disappeared, and the absorption spectra were in the range of 523 to 547 nm. Most electronic spectra come from the first transition S_0–S_1, corresponding to HOMO-1 to LUMO+1, HOMO to LUMO and LUMO to HOMO, Fig 4.

The maximum electronic transition energy values, E_T, of methylene blue are calculated as:

$$E_T = hcN_A/\lambda_{max} = 119626.8/\lambda_{max} \text{ (in nm) kJ/mol} \quad (1)$$

For investigated solvents and their binary aqueous mixtures, the values are listed in Table V. In fact, the electrostatic and non-electrostatic interactions between the solute and solvent molecules are included in the E_T values. The absorption maxima again shift to shorter wavelengths when the percentages of

the organic solvents increase in their aqueous binary mixtures, Table V. The changes are probably the result of the intermolecular solute–solvent interaction forces when the dielectric constant of the solutions decreases.

TABLE IV. The electronic spectra of methylene blue calculated in selected solvents at B3LYP/ 6-31+G* level

Solvent		Bond					
		S_0–S_1	S_0–S_2	S_0–S_3	S_0–S_4	S_0–S_5	S_0–S_6
Gas	MB	**500.61**	473.89	382.81	340.49	325.71	289.68
	MB–Cl	981.92	968.46	**670.93**	479.83	456.86	367.72
H_2O	MB	**536**.16	490.53	368.96	344.03	326.47	294.27
	MB–Cl	**536.72**	490.70	459.74	458.75	458.62	368.45
MeOH	MB	**535.79**	490.09	368.96	343.39	326.11	285.01
	MB–Cl	**536.75**	491.56	474.54	474.09	473.18	368.57
EtOH	MB	**537.75**	490.37	369.19	343.54	326.14	294.18
	MB–Cl	**538.81**	492.80	482.69	482.35	480.63	368.73
PrOH	MB	**539.12**	490.55	369.39	343.65	326.15	285.03
	MB–Cl	**547.07**	498.76	487.25	486.06	477.61	368.19
Dioxane	MB	**536.88**	485.69	376.43	343.50	326.21	293.51
	MB–Cl	959.77	952.96	918.85	**532.95**	483.07	369.42
Exp				660			

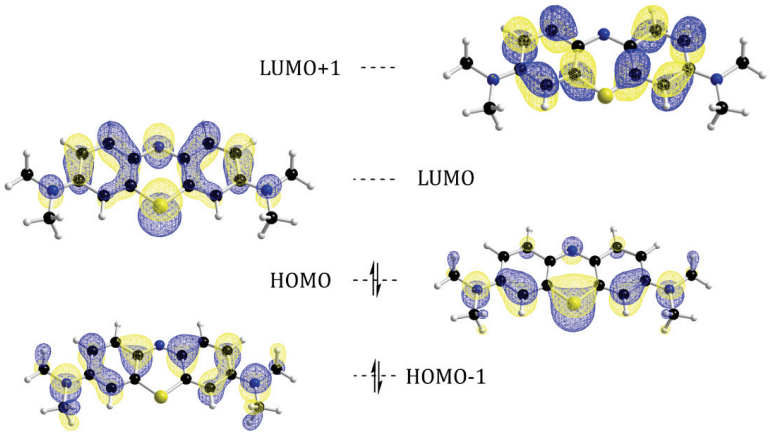

Fig. 4. The frontier orbitals of the MB optimized at B3LYP/6-31+G* in the gas phase.

TABLE V. Preferential solvation parameters of methylene blue in different aqueous binary mixtures at room temperature 25 °C; E_1 = 179.89 kJ mol^{-1}

Mixture	E_2 / kJ mol^{-1}	E_{12} / kJ mol^{-1}	$f_{2/1}$	$f_{12/1}$	$f_{12/2}$
H_2O–Dioxane	184.04	180.32	0.621	8.423	13.57
H_2O–PrOH	182.63	179.96	5.846	8.460	1.447
H_2O–EtOH	182.63	177.85	10.89	4.945	0.454
H_2O–MeOH	182.63	180.00	1.944	0.000	0.000

Fig. 5 presents the calculated E_T values of MB as a function of the mole fraction of the organic solvents. The ideal solvation behaviour of the mixtures can also be seen in the figure by the dashed line. Ideally, there is no preferential solvation between the solute and solvent molecules, and the composition of the solvent in the cybotactic region of the probe is the same as in the bulk solution. The apparent deviation from the linearity of E_T as a function of the mole fraction of the organic solvents shown in Fig. 5 can be interpreted as a preferential solvation of the probe by one of the components of the mixtures. Preferential solvation results from differences between the immediate surroundings of the solute and the bulk composition of the mixture. In fact, the non-linear behaviour of the E_T plots is due to the selective enrichment of a specific solvent species in the cybotactic region of the probe. The selective solvation results from the differences in the specific and non-specific interactions between the solute molecules and each of the solvent components.

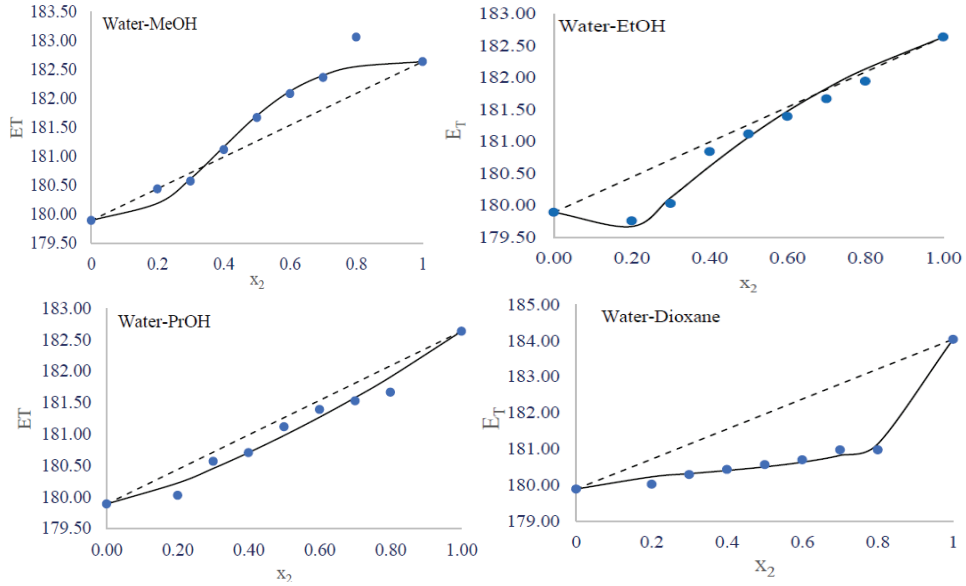

Fig. 5. Plots of the experimental and calculated E_T of MB versus the mole fraction of organic solvent: experimental values (filled circle), calculated values (solid line) and ideal values (dashed line).

The dependence of the E_T values of MB on the mole fraction of organic solvents shown in Fig. 5 are almost the same but with a significant difference from the dioxane values except for aqueous MeOH mixtures. The curves of MB E_T values show two different patterns, one in aqueous solutions of ethanol, propanol and dioxane and the other in water–MeOH mixtures. The E_T values for MB in

water with mixtures of ethanol, propanol and dioxane indicate selective solvation with the organic solvents. A negative deviation indicates that the MB is preferentially solvated in the solvent entities with a lower corresponding E_T. Regarding this account, the MB molecules are preferentially solvated by the organic solvent and the water–organic complexes resulting from solvent–solvent interactions. On the other hand, The E_T values have a sigmoidal dependence on the mole fraction of the organic solvent in water–MeOH mixtures. These observations indicate that in the water-rich region, MB molecules are preferentially solvated by water, while in the methanol-rich region, the MB molecules are selectively solvated with methanol molecules. In Fig. 5 there is a negative deviation from neat water up to $x_2 = 0.3$, Fig. 6, the local mole fractions of methanol in this region are lower than in water, indicating that MB is preferentially solvated by water due to hydrophobic hydration around the aromatic rings and methyl groups contributes to the negative deviation in methanol mixtures, this result is in agreement with results reported by Chen *et al.*[30] In Fig. 6, the compositions $0.3 < x_2 < 1$, the local mole fractions of methanol are greater than the values of water, leading to positive deviation, indicating that MB is preferentially solvated by methanol. The effect of cosolvents in increasing the solubility of the solute can be related to the disruption of the ordered structure of water around the polar moiety of methylene blue.

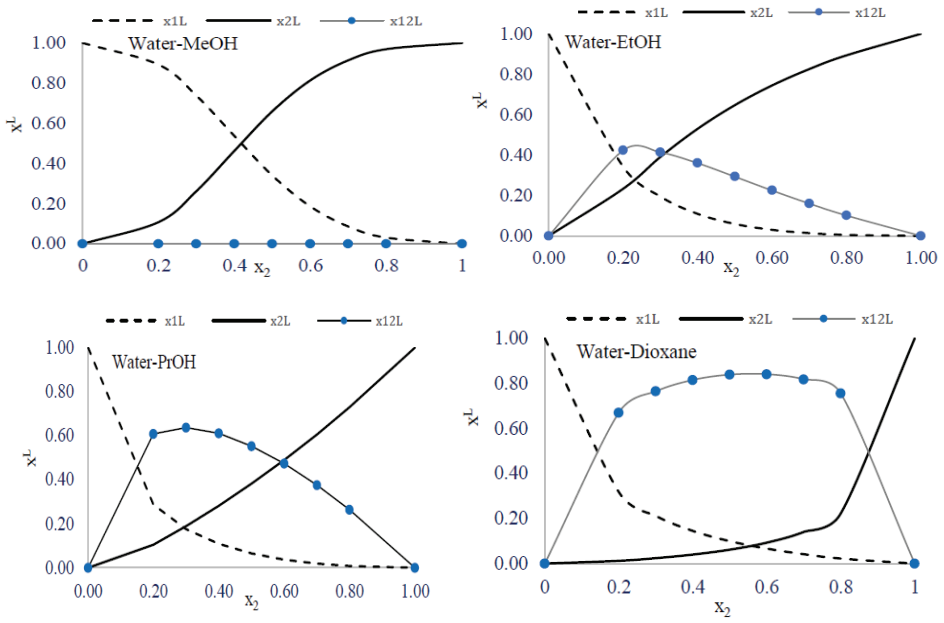

Fig. 6. Local mole fractions in the solvation shell of MB in various aqueous–organic systems at room temperature 25 °C.

Thus, the difference between the methanol, ethanol and propanol in the curve is reflected in the difference in the hydrogen bond donor (α), hydrogen bond acceptor (β) and hydrophobic properties of alcoholic solvents. Methanol is a higher hydrogen bond donor (0.93) and weaker hydrogen bond acceptor (0.62) than ethanol (α = 0.83, β = 0.77) and propanol (α = 0.84, β = 0.85). The hydrophobicity of ethanol and propanol is also higher than that of methanol. Thus, ethanol, in comparison with methanol, has a much greater tendency to solvate acidic and hydrophobic molecules such as MB, which preferentially occurs in water-rich environments. This means that when methanol is replaced by ethanol or propanol, the preferential solvation of the solute increases to more extent by an alcoholic solvent. In other words, in the HBD solvents, the hydrogen bonds between the dimethyl amino group of the dye and, thus, the OH group in the solvents play an important role in the solvation of the dye. The interaction of the hydroxyl solvent with other components of the mixture can lead to the formation of hydrogen-bonded complexes that solvate the less polar part of the dye, *i.e.*, alkyl groups present in the solvents.[31] Based on the strong interaction between the dioxane and water molecules, the behaviour of the mixture is different compared to water–alcohol solutions. The hydrogen bond between dioxane and water molecules is stronger than water–water. The presence of dioxane molecules significantly destroys the net structure of water, and therefore, water-dioxane complexes are the dominant species in the preferential solvation of the solute over the whole range of mole fractions of dioxane, Fig. 6.

Analysis of data in binary aqueous systems by the preferential solvation parameters

To describe the solvation, we need to consider the preferential solvation parameters listed in Table V. The preferential solvation parameters, $f_{12/1}$ and $f_{2/1}$, show the tendency of the solute to be solvated by S_{12} and S_2 in preference of the solvent S_1, respectively, and the $f_{12/2}$ parameter measures the preferential solvation of the solute by S_{12} relative to solvent S_2. If $f_{12/1}$ and $f_{12/2}$ are higher than unity, then this will demonstrate that the solute tends to be solvated by S_{12} (water–organic solvent complex) rather than by the pure solvents.[32]

Observing the results in Table V for the MB in the alcoholic solutions, the results show that the $f_{2/1}$ parameter is higher than unity in the order ethanol > propanol > methanol, suggesting that the MB molecules are preferentially solvated with alcohol molecules and water–alcohol complexes formed by solvent––solvent interactions. The value of $f_{2/1}$ is higher than $f_{12/2}$ in aqueous mixtures of ethanol and propanol, indicating that the order of preferential solvation in these mixtures is $S_2 > S_{12} > S_1$. In addition, the parameter $f_{12/1}$ is greater than $f_{12/2}$, which indicates that the nature of the complex is closer to that in water than in alcohols for ethanol and propanol mixtures. The local mole fraction of the com-

plex solvent reaches a maximum of approximately x_2 in aqueous mixtures of 0.2–0.3 ethanol and 0.2–0.5 propanol. As it can clearly be seen in Fig. 6, the solvation shell of MB is fully saturated with protic solvent and a complex solvent over the whole composition range. This result is consistent with the molecular structure of MB, Fig. S-1, because MB has several amino groups in its structure, which makes the solute able to protonate from the solvent by forming HB with amino groups. Therefore, the values of $f_{12/1}$ and $f_{12/2}$ in aqueous propanol solutions are higher than in aqueous ethanol solutions, indicating that the water–propanol complex plays a significant role in the solvation of the probe.

A different scenario is observed for water–MeOH mixtures with zero values of $f_{12/1}$ and $f_{12/2}$. These results indicated that the solvated complex species formed by water–methanol interaction could not be incorporated into the solvation shell of MB with respect to the methanol and water. As mentioned, the hydrogen bond between the lone pair electrons of nitrogen and the hydrogen bond donor of the solvent cause its unstable form. In this case, the solvation of MB is favoured thermodynamically in solvents with lower hydrogen bond donor capacity. Based on this result, the water–MeOH aggregates have better hydrogen donating ability than MeOH, because E_{T12} is close to E_{T1}, indicating that the complex is closer in nature to water than to methanol; thus, the preferential solvation by MeOH molecules is favoured in MeOH-rich region. Therefore, as indicated by the preferential solvation parameters, the preferential solvation extent of MB increases as the solvent becomes less of a hydrogen bond donor.

In the case of dioxane as an aprotic solvent (HBA), $f_{2/1}$ has a small value, and $f_{12/1}$ and $f_{12/2}$ are higher than unity, Fig. 6. However, the E_T values of the MB have a negative deviation depending on the dioxane mole fraction, Fig. 5. In this case, the $f_{12/2}$ has the highest value and is significantly different from the other preferential solvation parameters. This observation indicates that in the water-rich region, the MB molecules are preferentially solvated by water molecules, while in the dioxane-rich region, the MB molecules are mainly solvated by the dioxane–water complex molecules. Also, the higher value of $f_{12/2}$ than $f_{12/1}$ indicates that the nature of the dioxane–water complex molecules is closer to dioxane than to water molecules. The preferential solvation order of aqueous dioxane solutions is $S_{12} > S_2 > S_1$. These results, supported by the local mole fraction of the complex solvent, reach a maximum between the range of 0.2 and 0.8. As shown in Fig. 6, the solvation shell of MB is fully saturated with the solvent complex and dioxane over the whole composition range. Table I shows that the E_T values of S_{12} (E_{12}) are lower than the E_{T2} and higher than the E_{T1} in aqueous dioxane mixtures, indicating that the β-basicity of the solvated species increases in the order $S_{12} > S_2 > S_1$. Therefore, in the competition between S_2 and S_{12}, the MB molecules preferentially interact with S_{12} due to stronger hydrogen bonding interactions, resulting in the $f_{12/2} > 1$. This means that in the dioxane

binary mixture, the difference between the basicity of S_2 and S_{12} confirms the increasing order of the $f_{12/2}$ shown in Table V.

Analysis of spectral data in binary aqueous systems with the KAT polarity scale

The changes of the obtained E_T values with the solvents used, Table V, reveal that the solute–solvent interactions between the methylene blue and the solvent molecules depend on specific and non-specific interactions. The method introduced by Kamlet, Abboud and Taft (KAT) is used to quantify these interactions.[33] This approach has been successfully applied in correlation analysis of all kinds of solvent-dependent processes.[4] The multi-parametric KAT equation has been introduced in previous reports:[9,15,18]

$$E_{T(MB)} = E_{T(o)} + a\alpha + b\beta + s\pi^* \quad (2)$$

Where $E_{T(o)}$ represents the regression value, the π^* is the index of the solvent dipolarity/polarizability, which is a measure of the ability of a solvent to stabilize a charge or a dipole by its dielectric effects. The α coefficient represents the solvent hydrogen-bond donor (HBD) acidity. In other words, it describes the ability of a solvent to donate a proton in a solvent to a solute hydrogen bond. The β coefficient is a measure of solvent hydrogen-bond acceptor (HBA) basicity and describes the ability of a solvent to accept a proton from a solute molecule. The regression coefficients a, b and s measure the relative susceptibilities of the solvent dependence of E_T. The E_T values were correlated with solvent properties by means of single, dual and multiple regression analysis by a suitable computer program.[18] Gauss–Newton non-linear least-squares method in the computer program is used to refine the values of E_T by minimizing the error squares sum:

$$U = (E_{T,exp} - E_{T,cal})^2 \quad (3)$$

The number of terms in the KAT equation used to correlate the studied property depends on the significance of the solute–solvent interactions.

In the study, several attempts are made to find the best form of the KAT equation to describe the variation of E_T values in the water–organic solvent mixtures. So, a stepwise procedure and least squares analysis were applied to select the significant solvent properties to be influenced in the model and to obtain the final expression for E_T. Therefore, the KAT equation was used as single, dual and multi-parameter forms for correlation analysis of E_T in various solvent mixtures. The computer program used can also give the values of $E_{T(o)}$, a, b, s and some statistical parameters, including the r^2 coefficient, uncertainty value of each parameter (given in brackets) and residual sum of squares (*rss*). The KAT parameter values for all the aqueous organic mixtures used in this work were obtained from the values reported in the literature[18] and are listed in Table S-I.

The most significant resulting regression equations describing the correlation between E_T and the KAT parameters for MB are shown in Table VI.

TABLE VI. Coefficients of LSER equation for MB in the binary systems and statistical parameters; *b* and *s*: coefficients; *R*: correlation coefficients; *F*: Fisher number; *p*: the probability of variation; *SD*: standard deviation; *rss*: residual sum of squares

System	$E_{T(o)}$	*b*	*s*	*R*	*F*	*SD*	*rss*	*p*
Water–dioxane	189.09±1.49	–9.80±2.28	–3.383±0.77	0.92	17.10	0.55	1.8	3×10^{-3}
Water–PrOH	180.61 ±1.08	3.596±0.89	–2.191±0.55	0.99	157.8	0.14	0.1	6×10^{-6}
Water–EtOH	185.54±0.96	–0.480±1.05	–5.080±0.41	0.99	167.1	0.15	0.1	5×10^{-6}
Water–MeOH	184.27±1.39	3.176±1.54	–5.319±0.72	0.97	42.76	0.32	0.6	3×10^{-4}

The analysis of the absorption bands in neat solvents by KAT parameters was conducted to find the best descriptive model. The multi-parametric analysis, including α, β and π^* terms by using LSER is shown in Eq. (4), with a correlation coefficient, $r = 0.999$) and the highest *F*-value = 955.002:

$$E_{T(MB)} = 188.251 - 0.552\alpha - 2.40\beta - 6.043\pi^* \quad (4)$$

From the analysis of the result in Eq. (4), the hydrogen bonding acceptance ability and the dipolarity/polarizability are more evident for the spectral shift. A significant contribution of α to MB solvatochromism is not observed alone or in combination with other terms. The negative sign and the magnitude of β and π^* in Eq. (4) show that both solvent dipolarity/polarizability and hydrogen-bonding basicity affect the spectral shift with different strengths. Based on this result, the dual-parametric KAT-LSER is the best descriptive model with β and π^* parameters in all binary mixtures. Compared to Eq. (4), the regression coefficients are changed, and the correlation coefficient decreased, especially for aqueous dioxane mixtures, due to the complexity of interactions between the solute and the solvent molecules in the mixed solvents. The main contributions to this complexity stem from the non-ideality of the solution due to solvent–solvent interactions and the preferential solvation due to different interactions of the solute with solvents in each mixture. The analysis of the coefficients in Table VI shows that the spectrum shifts becomes more sensitive to the value π^* of the medium in aqueous methanol and ethanol mixtures, while in aqueous propanol and especially in aqueous dioxane mixtures, the effect of β becomes more evident. It should be noted that the magnitude of the coefficients for aqueous methanol, ethanol and propanol differs from that in Eq. (4) for mono-solvents; the correlation coefficient of the KAT-LSER model was found to be greater than 0.96. The spectral change in this mixed solvent turns out to follow a linear relationship with the polarity (explained by β and π^*) similar to that of mono-solvents. These observations indicate that the nonlinearity in the spectral shifts, when plotted as a function of mole fraction, is due to the non-ideality of the polarity of these binary systems,

rather than to the preferential solvation with a single solvent. For more clarification, we use β and π^* of binary mixtures present to calculate E_T as a function of composition using Eq. (2). Non-ideality of mixtures is reflected in the compositional dependence of β and π^* of mixtures; therefore, Eq. (2) gives an estimation of the solute's spectral response to solvent composition change when the polarity of solvation shell and bulk is the same as the result of the absence of preferential solvation. When plotting the observed E_T against the estimated values from Eq. (2) in Fig. 7. Clearly, high linear correlations (r^2 = 0.93) with a slope close to unity and intercept close to zero are obtained between two sets of data in methanol, ethanol, and propanol binary systems. This evidence shows that the polarity of the solvation shell experienced by the solute differs just slightly from that of the bulk, which in turn results in insignificant compositional differences between the local and bulk environments.[34] This result is in discordance with the one obtained from solvation model analysis, which reveals the significant contribution of preferential solvation to solvatochromism in water with methanol, ethanol and propanol binary mixtures. The latter is well justified by $f_{2/1}$ = 1.944, 10.89 and 5.896, respectively, calculated by the proposed model in this work, which shows very high preferential solvation by cosolvents. Fig. 7 displays a notable departure from the bisector line that is directly indicative of the occurrence of preferential solvation in the case of the dioxane binary system. As the main result, the non-ideality of solvent mixtures has a significant influence on the

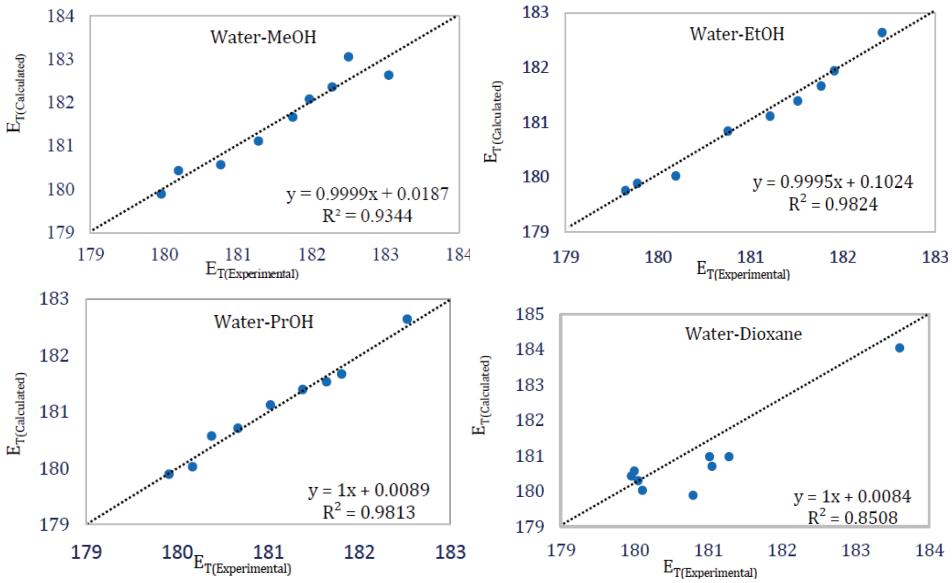

Fig. 7. Plots of correlation of the observed E_T with the estimated E_T using Eq. (2) in the absence of the solute's preferential solvation in aqueous mixtures of methanol, ethanol, propanol and dioxane at 25 °C, dotted lines show the bisector of the first quadrant.

spectral response of the solute related to the local composition and the preferential solvation from the analysis of non-linear solvatochromism. Finally, from Table VI, it is noted that the sign of π^* coefficient is negative in all binary systems, indicating the negative polarity contribution to the spectral shift of MB by a strong contribution of hydrogen bonding interaction of MB with the solvent entities. Interestingly, the β coefficient also has a positive sign in some binary systems, unlike the sign in mono solvents. This unexpected result originates from the different forms of interactions in mixed solvents because the interactions in mixed solvents are more complex than those in pure solvents.

CONCLUSIONS

The spectroscopic behaviour in binary solvent mixtures was analysed using the preferential solvation approach. The obtained results show that the λ_{max} values were blue-shifted to shorter wavelengths as the relative permittivity of the solutions decreases. Although the hydrogen bonding donor acidity of water is highest among the mixture constituents, the downward curvature of the E_{T12} value *versus* the analytical mole fraction of cosolvents indicates that the MB is more solvated by the cosolvent components except in methanol mixtures. It was discussed whether the self-association of water molecules to make network structure is responsible for the reduction of the water affinity to compete with the other solvating species. The solvent exchange model was perfectly fitted to the observed E_T values. The preferential solvation parameters were calculated from the model. The results demonstrate that the solution behaviour of MB in the studied mixtures can be adequately explained by the competition of solvating species to interact with the MB through hydrogen bonding interactions. In a water–methanol mixture, the affinity of S_2 and S_1 to the solvation of MB is $S_2 > S_1$, whereas S_{12} species do not play a role in the solvation of MB, while in the ethanol and propanol mixtures, the solvent species preferentially solvates the solute in order $S_2 > S_{12} > S_1$. In the case of water with dioxane, a different order is observed: $S_{12} > S_2 > S_1$ over the whole range composition.

The molar transition energy of MB in different binary mixtures was analysed in terms of the KAT equation. Dual-parameter correlations showed better results in the HBD solvents and dioxane as HBA solvents, respectively. The correlation of E_{T12} with the KAT parameters showed that the polarity/dipolarity which had more impact in the case of aqueous methanol and ethanol mixtures was responsible for the solvatochromism observed in the absorption spectra of MB, whereas the hydrogen bond accepting ability in the case aqueous of propanol and dioxane mixtures was more responsible for the solvatochromism observed in the absorption spectra of MB. A dramatic deviation from linearity in solvatochromism was observed, which is mainly due to the combined effect of solution non-ideality and preferential solvation.

SUPPLEMENTARY MATERIAL

Additional data and information are available electronically at the pages of journal website: https://www.shd-pub.org.rs/index.php/JSCS/article/view/12388, or from the corresponding author on request.

Acknowledgment. The authors are grateful to Dr. Ali Farajtabar for his scientific help in this investigation.

ИЗВОД

ДОПРИНОС НЕИДЕАЛНОГ ПОНАШАЊА БИНАРНИХ ВОДЕНИХ СИСТЕМА РАЗЛИЧИТИМ СВОЈСТВИМА РАСТВАРАЧА ИНКОРПОРИРАНИХ У СОЛВАТАЦИОНУ ЉУСКУ МЕТИЛЕНСКО ПЛАВОГ

SOKAINA S. HEMDAN[1] и RADWAN ALNAJJAR[2,3]

[1]Department of Chemistry, Faculty of Science and Art El Marj, Benghazi University, El Marj, Libya, [2]Department of Chemistry, Faculty of Science, Benghazi University, Benghazi, Libya и [3]PharmD, Faculty of Pharmacy, Libyan International Medical University, Benghazi, Libya

Солватохромна својства метиленско плавог (МВ) испитивана су у чистим растварачима: води, метанолу, етанолу, пропанолу и диоксану, као и њихивом воденим смешама. Испитивана је корелација вредности емпиријске скале поларности растварача (ET) за МВ са саставом растварача коришћењем Bosch и Roses модела измене растварача да би се објаснило преференцијално растварање одабране тиазинске боје у бинарним мешаним растварачима. Нелинеарни солватохромизам МВ је опажен у воденим смешама метанола, етанола, пропанола и диоксана. Утицај састава на солватациону љуску при преференцијалном растварању МВ је испитиван са аспекта растварач–растварач и растворак–растварач интеракција и израчуната је локална молска фракција састава сваког растварача у непосредној околини растворка МВ. Варијације ефективне молске фракције могу дати важан физичкохемијски увид у микроскопске и молекулске интеракције између МВ и компоненти растварача. Резултати показују да је солватациона љуска МВ више засићена комплексом растварача S_{12} у случају диоксана у односу на смеше етанола и пропанола, а супротан тренд је детектован за смеше метанола, с обзиром на то да комплекс растварача S_{12} није могао да се инкорпорира у МВ солватациону љуску. Подаци бинарних система су анализирани КАТ параметрима коришћењем дуалног модела базности и поларности. Добијени резултати су показали да поларност више одговара за опис спектралног помераја у воденим растворима метанола и етанола, док је базност прикладнија за водене растворе пропанола и диоксана.

(Примљено 12. маја, ревидирано 18. јуна, прихваћено 1. новембра 2023)

REFERENCES

1. C. Reichardt, T. Welton, *Solvents and Solvent Effects in Organic Chemistry.* Wiley-VCH, Weinheim, 2011 (http://dx.doi.org/10.1002/9783527632220)
2. A. M. Al-Jebaly, S. S. Hemdan, F. K. Ali, *J. Sci. Hum. Studies* **39** (2017) 1 (http://dx.doi.org/10.37376/1571-000-039-003)
3. N. Elmsheeti, S. Hemdan, A. Sammour, R. Alnajjar, *Chem. Data Collect.* **28** (2020) 100465 (https://doi.org/10.1016/j.cdc.2020.100465)
4. M. S. Masoud, R. I. M. Elsamra, S. S. Hemdan, *J. Serb. Chem. Soc.* **82** (2017) 856 (http://dx.doi.org/10.2298/JSC170204032M)

5. A. M. Al-Jebaly, S. S. Hemdan, F. K. Ali, *J. Natur. Sci., Life Appl. Sci.* **1** (2017) 33 (http://dx.doi.org/10.26389/AJSRP.A071217)
6. S. Hemdan, A. Al Jebaly, F. Ali, *Acad. J. Res. Sci. Pub.* **2** (2021) 28 (http://dx.doi.org/10.52132/Ajrsp.e.2021.242)
7. J. Catalán, C. Dıaz, F. Garcıa-Blanco, *J. Org. Chem.* **65** (2000) 9226 (http://dx.doi.org/10.1021/jo001008u)
8. D. C. Da Silva, I. Ricken, M. A. D. R. Silva, V. G. Machado, *J. Phys. Org. Chem.* **15** (2002) 420 (http://dx.doi.org/10.1002/poc.519)
9. S. S. Hemdan, *J. Solution Chem.* (2023) (http://dx.doi.org/10.1007/s10953-023-01301-3)
10. R. I. Stock, L. G. Nandi, C. R. Nicoleti, A. D. S. Schramm, S. L. Meller, R. S. Heying, D. F. Coimbra, K. F. Andriani,G. F. Caramori, A. J. Bortoluzzi, V.G. Machado, *J. Org. Chem.* **80** (2015) 7971 (http://dx.doi.org/10.1021/acs.joc.5b00983)
11. A. Farajtabar, F. Jaberi, F. Gharib, *Spectrochim. Acta A* **83** (2011) 213 (http://dx.doi.org/10.1016/j.saa.2011.08.020)
12. O. A. El Seoud, *Pure Appl. Chem.* **79** (2007) 1135 (http://dx.doi.org/10.1351/pac200779061135)
13. A. Ben-Naim, *J. Phys. Chem.* **93** (1989) 3809 (http://dx.doi.org/10.1021/j100346a086)
14. Y. Marcus, *J. Chem. Soc. Faraday Trans. 1* **84** (1988) 1465 (http://dx.doi.org/10.1039/F19888401465)
15. P. Suppan, *J. Chem. Soc. Faraday Trans. 1* **83** (1987) 495 (http://dx.doi.org/10.1039/F19878300495)
16. F. Gharib, A. Shamel, F. Jaberi, A. Farajtabar, *J Solution Chem.* **42** (2013) 1083 (http://dx.doi.org/10.1007/s10953-013-0007-9)
17. R. D. Skwierczynski, K. A. Connors, *J. Chem. Soc. Perkin Trans. 2* (1994) 467 (http://dx.doi.org/10.1039/P29940000467)
18. S. S. Hemdan, A. M. Algebali, F. K. Ali, *J. Chem. Technol. Metall.* **58** (2023) 125 (https://journal.uctm.edu/node/j2023-1/JCTM_2023_58_15_22-77_pp125-142.pdf)
19. J. P. Perdew, *Phys. Rev., B* **34** (1986) 7406 (https://dx.doi.org/10.1103/PhysRevB.33.8822)
20. T. Yanai, D. P. Tew, N. C. Handy, *Chem. Phys. Lett.* **393** (2004) 51 (https://dx.doi.org/10.1016/j.cplett.2004.06.011)
21. J. Chai, M. Head-Gordon *Phys. Chem. Chem. Phys.* **10** (2008) 6615 (https://dx.doi.org/10.1039/B810189B)
22. A. Austin, G. A. Petersson M. J. Frisch, F. J. Dobek, G. Scalmani, K. Throssell, *J. Chem. Theory Comput.* **8** (2012) 4989 (https://dx.doi.org/10.1021/ct300778e)
23. M. Walker, A. J. A. Harvey, A. Sen, C. E. H. Dessent, *J. Phys. Chem., A* **117** (2013) 12590 (https://dx.doi.org/10.1021/jp408166m)
24. Y. Takano, K. N. Houk, *J. Chem. Theory Comput.* **1** (2005) 70 (https://dx.doi.org/10.1021/ct049977a)
25. N. Elmsheeti, S. Hemdan, A. Sammour, R. Alnajjar, *Chem. Data Collect.* **28** (2020) 100465 (https://dx.doi.org/10.1016/j.cdc.2020.100465)
26. *Gaussian 16, revision C. 01*., 2016
27. Sabirov V. Kh. Vahobjon CCDC 2223592: Experimental Crystal Structure Determination, 2022 (https://doi.org/10.5517/ccdc.csd.cc2dmtsn)
28. S. S. Hemdan, *J. Fluoresc.* (2023) (http://dx.doi.org/10.1007/s10895-023-03234-y)
29. H. C. Boroujeni, F. Gharib, *J. Solution Chem.* **45** (2016) 95 (https://doi.org/10.1007/s10953-015-0425-y)

30. X. Chen, A. Farajtabar, W. Jia, H.Zhao, *J. Chem. Thermodyn.* **138** (2019) 179 (https://doi.org/10.1016/j.jct.2019.06.019)
31. T. Bevilaqua, T. F. Goncalves, C. G. Venturini, V. G. Machado, *Spectochim. Acta, A* **65** (2006) 535 (http://dx.doi.org/10.1016/j.saa.2005.12.005)
32. M. Rosés, C. Ràfols, J. Ortega, E. Bosch, *J. Chem. Soc. Perkin Trans. 2* (1995) 1607 (http://dx.doi.org/10.1039/P29950001607)
33. R.W. Taft, J.L.M. Abboud, M.J. Kamlet, *J. Org. Chem.* **49** (1984) 2001 (http://dx.doi.org/10.1021/jo00185a034)
34. X. Yao , R. Fang, H. Zhao , A.Farajtabar, A. Jouyban ,W.E. Acree Jr, *J. Mol. Liq.* **349** (2022) 118515 (http://dx.doi.org/10.1016/j.molliq.2022.118515).